Theoretical study on the photostimulated desorption of CO from a Pt surface

H. Nakatsuji
Department of Synthetic Chemistry and Biological Chemistry, Faculty of Engineering, Kyoto University, Sakyo-ku, Kyoto 606-01, Japan and Institute for Fundamental Chemistry, 34-4, Tankano-Nishihiraki-cho, Sakyo-ku, Kyoto 606, Japan

H. Morita and H. Nakai
Department of Synthetic Chemistry and Biological Chemistry, Faculty of Engineering, Kyoto University, Sakyo-ku, Kyoto 606-01, Japan

Y. Murata and K. Fukutani
Institute for Solid State Physics, University of Tokyo, Roppongi, Minato-ku, Tokyo 106, Japan

(Received 8 May 1995; accepted 3 October 1995)

Photostimulated desorptions (PSD's) of CO, CO^+, and CO^- from a Pt surface are studied theoretically using Pt_2–CO model cluster including image force correction. Calculations are performed by the single excitation configuration interaction and the symmetry adapted cluster (SAC)/SAC-CI methods. The PSD's of the ground state CO occur as the Menzel–Gomer–Redhead (MGR) process and those of CO^+ (n cation) and excited ($n \rightarrow \pi^*$) CO* through the modified MGR process in which the upper repulsive potential curves are nonadiabatic; the process proceeds through a sequence of nonadiabatic transitions between the similar pertinent states embedded in the metal excited bands. The excited states as the desorption channels are characterized by the excitations from the Pt–CO bonding orbitals to the antibonding MO's: metal-adsorbate chemical bond cleavage by photons which leads to a repulsive potential is essential for the PSD. The electrostatic image force interaction plays only a minor role and the present result does not support the Antoniewicz model. The calculated excitation-energy thresholds for the CO, CO^+, and CO* desorptions are 1.6~2.6, 11.3, and 11.3–12.7 eV, respectively, which explains the energy thresholds and the fluence dependencies of the incident laser in the PSD experiments. On the other hand, the PSD giving CO^- would occur with the energy range of 6.2–8.2 eV, one to two photon energy of the 193 nm (6.4 eV) laser. Since the upper nonadiabatic potential curves have shallow minima, in this case, the lifetime of the CO^- species would be larger than those of the CO^+ and CO* species. The present study clarifies the electronic structures of the desorbed CO^+, CO^-, and CO* species, which have not been identified experimentally. [S0021-9606(96)01102-1]

I. INTRODUCTION

Surface photochemistry is a newly developing field in surface chemistry and photochemistry.[1] Recently, much effort has been devoted to clarify molecular processes in surface photochemical reactions, such as photodissociations and photostimulated desorptions (PSD). The PSD may involve many complicated phenomena; photoabsorption by admolecule and/or surface, energy and electron transfers between them, and energy redistributions into internal degrees of freedom of the surface and the desorbed molecule. Clarifications of the electronic mechanisms of these processes are very important for understanding and designing specific photocatalytic reactions on a solid surface.

Murata and co-workers have studied the mechanisms of ultraviolet PSD's of NO (Refs. 2–5) and CO (Refs. 5–7) from Pt(001) and Pt(111) surfaces. The experiment for the CO/Pt(001) system with the use of 193 nm (6.4 eV) UV laser gave both CO and CO^+ photodesorptions, while no desorption was observed by the 248 and 352 nm (5.0 and 3.5 eV) UV lasers. The PSD yields of CO and CO^+ species exhibit third- and second-order dependencies, respectively, on the laser fluence. On the other hand, the PSD yields of CO and CO^+ from the Pt(111) surface show first- and third-order dependencies, respectively, and the energy threshold for the CO desorption was observed at 2.7 eV.[8] On the other hand, the PSD experiments of CO on Ni(111)/O (Ref. 9), W (Ref. 10), and Cu(111) (Ref. 11) surfaces gave the desorptions of only neutral CO species.

On the theoretical side, Menzel, Gomer, and Redhead[12,13] (MGR) proposed a two-step mechanism for the PSD: the first step is the Franck–Condon transition from the ground to the excited states of the admolecule-surface system, which is induced by the absorption of photon energy. In the second step, the admolecule moves out from the surface along the *repulsive* potential energy curve of the excited state. While this qualitative MGR model is very simple and acceptable by intuition, we wonder whether there exists a *unique* repulsive curve in actual surface-molecule interacting systems. Antoniewicz,[14] on the other hand, proposed another model, which involves photoexcited ionic intermediate. In his model, the van der Waals (vDW) and image force (IF) interactions are considered important as surface-molecule interactions, and the surface-adsorbate distance is assumed to become small as the charged intermediate is assumed to be

 0021-9606/96/104(2)/714/13/$6.00

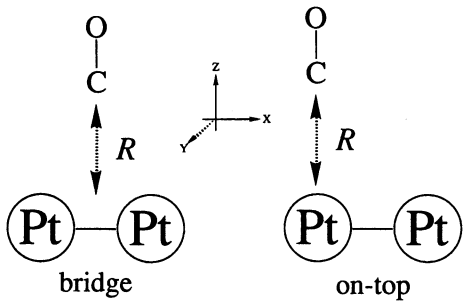

FIG. 1. Geometries of the model Pt_2–CO systems.

involved in the PSD process. However, as shown later, the adsorption of CO onto a Pt surface is due to a usual chemical bond, which is stronger than the vDW and IF interactions in short distances, we wonder whether the Antoniewicz model can be applied to the PSD of CO from the Pt surface.

Several *ab initio* molecular orbital (MO) calculations have been carried out for the interactions between the CO and Pt surface. For example, Smith and Carter carried out the generalized valence bond (GVB) calculation for the lowest three states of a linear Pt–CO system.[15] The ground $^1\Sigma^+$ state of PtCO is led from the excited ^1S state of Pt, which formally has a $d^{10}s^0$ valence electron configuration. The Pt–CO bond is formed mainly by the σ donation from the lone pair nonbonding (n) MO of CO to the vacant $6s$ AO of Pt and by the π back donation from the $5d$ AO of Pt to the vacant π^* MO of CO. While the calculation describes well the adsorption of CO, no results have been reported on the excited states corresponding to the PSD experiments.

Nakatsuji and co-workers have studied several surface reactions theoretically, using the cluster model and the dipped adcluster model (DAM).[16,17] The electron correlations and excited states necessarily considered for surface phenomena were calculated using the symmetry adapted cluster[18] (SAC)/SAC-configuration interaction[19] (SAC-CI) method.[20,21] The systems studied are H_2/Pd,[22] C_2H_2/H_2/Pd,[23] H_2/Pt,[24] O_2/Pd,[16,17] H_2/ZnO,[25] O_2/Ag,[26–28] Cl_2/K, Na, Rb,[29] H_2/ZrO_2,[30] and HCOOH/MgO.[31] Our purposes have been to develop the methodology for studying surface reactions and to clarify the electronic mechanisms involved in these surface-molecule interaction systems. In particular, we have clarified the mechanisms of the harpooning, the surface chemiluminescence and electron emission for the Cl_2/K, Na, Rb systems, which may be considered as a junction between surface chemistry and surface photochemistry.[29]

In the present study, the purpose is to clarify the electronic mechanism of the PSD of CO from a Pt surface. The surface is represented by a Pt_2 cluster and the electronic structures of the ground and many excited states of the Pt_2CO system are calculated by *ab initio* Hartree–Fock (HF)/single excitation CI (SECI) and SAC/SAC-CI methods.

II. COMPUTATIONAL DETAIL

In this study, we use the Pt_2–CO system shown in Fig. 1 as a model; the bridge site model has C_{2v} symmetry and the on-top site model has C_s symmetry. The effect of the electrostatic image force between the adsorbate and the extended surface is incorporated for each ground and excited states by the method proposed previously.[17] The size of the cluster, Pt_2, is small, even though we may assume the locality of the interaction between the admolecule and the surface. We have to be careful, therefore, to the results which are dependent on the size of the cluster.

The potential energy curves of the ground and excited states are calculated as a function of the distance R between Pt_2 and CO. The CO axis is fixed to be perpendicular to the Pt_2 axis, and the CO distance is fixed to be 1.1283 Å, which is the equilibrium distance of the free molecule.[32] The Pt–Pt distance is also fixed at 2.7746 Å, which is the lattice distance in a solid platinum.[33]

The Gaussian basis set for the platinum atom is $(3s3p3d)/[3s2p2d]$ and the Xe core was replaced by the relativistic effective core potential.[34] For carbon and oxygen, we use the $(9s5p)/[4s2p]$ set of Huzinaga–Dunning[35] augmented by the polarization d functions of $\alpha_C=0.600$, and $\alpha_O=1.154$, respectively.

The ground and excited states of the Pt_2–CO system are calculated by the HF/SECI and SAC/SAC-CI methods. The HF calculations were carried out with the use of the program HONDO8.[36] The program system SAC85 (Ref. 37) was used for the SECI and SAC/SAC-CI calculations. The active space consists of 15 occupied and 53 unoccupied HF orbital space. Only the two occupied core orbitals, which are $1s$ AO's of C

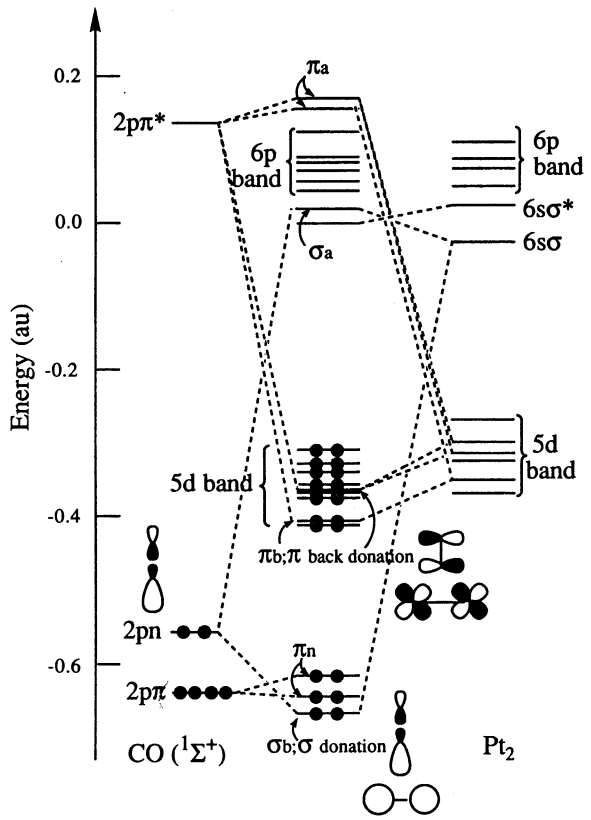

FIG. 2. A schematic orbital correlation diagram for the interaction between CO and Pt_2 in the bridge-site adsorption.

and O, and their counterparts in the vertical space are frozen. To reduce the size of the matrices involved, the configuration selection is made as reported previously.[20] For the ground and excited states, the thresholds are set to 7×10^{-5} and 1×10^{-4} a.u., respectively.

III. ADSORPTION OF CO ON A Pt SURFACE

In the ground state, both the bridge and on-top sites are bound. The equilibrium Pt_2–CO distance is calculated to be 1.44 Å for the bridge site and 1.90 Å for the on-top site. The surface-CO distance of the bridge form is calculated to be 0.47 Å shorter than that of the on-top form. At the HF level, the bridge form is calculated to be more stable than the on-top form, which may contradict with the experimental result. This is perhaps due to the very small size of the cluster model used here.

We investigate the bonding between Pt_2 and CO. The basic interaction is quite similar between the bridge and on-top geometries. As in usual metal–carbonyl compounds, the Pt_2–CO bond is mainly due to the σ donation and the π back donation. As shown in the orbital correlation diagram, Fig. 2, shown for the bridge form, the electron in the nonbonding $p(n)$ orbital of CO is donated to the $6s\sigma$ MO of Pt_2 and those in the $5d\delta^*$, $5d\pi^*$, and $5d\sigma^*$ MO's of Pt_2 are back donated to the π^* MO's of CO. The bonding and antibonding MO's of these interactions are denoted by σ_b, π_b, and σ_a, π_a, respectively, in Fig. 2. Note that the σ_a MO, which consists of the $6s\sigma$ orbital of Pt_2 and the n orbital of CO, is higher in energy than the $6s\sigma^*$ MO of Pt_2 of the adsorbed system. The π MO's of CO are well localized in the Pt_2–CO system and are denoted as π_n.

Table I shows the population analysis of the Pt_2–CO system in the adsorbed and separated forms calculated by the SAC/SAC-CI method. The donations and back donations of electrons are confirmed by examining the populations for the $^1A_1$ state. The Pt(s) population increases from 0.107 to 0.528 (difference 0.421) by the adsorption of CO, while those of the d_{xx} and d_{xz} orbitals decrease by 0.174 and 0.282, respectively. On the other hand, the $C(s)$ and $C(p_z)$ populations decrease by 0.583 and 0.117, respectively, and the $C(p_x)$ and $C(p_y)$ ones increase by 0.177 and 0.122, respectively. Table I also shows that the oxygen orbital populations do not change much as the carbon and platinum ones and that the in-plane interaction between Pt_2 and CO is larger than the out-of-plane one.

The total charge of CO of the adsorbed Pt_2–CO system is +0.231 implying that the σ donation is larger than the π back donation. Furthermore, this charge is smaller than those in the adsorptions of oxygen[26–28] and halogen[29] molecules, so that the system may be studied without using the dipped adcluster model.[16] This is why we use the cluster model in the present study. However, we note that we have included the image force correction[17] in the present calculations.

IV. PSD OF CO FROM A Pt SURFACE

A. Adiabatic and nonadiabatic potential curves of the excited states at the HF/SECI level

We investigate the potential energy curves (PEC's) of the Pt_2–CO system as a function of the Pt_2–C distance, R. The upper left side of Fig. 3 shows the PEC's for the ground and lower 90 $^1A_1$ excited states, whose excitation energies are lower than 24 eV, calculated at the HF/SECI level. They are obtained for the bridge adsorption form and the similar curves for the $^1A_2$, $^1B_1$, and $^1B_2$ states are also shown in Fig. 3 together with the ground state ($^1A_1$) curve. Figure 3 shows that the adiabatic PEC's of this system are so dense

TABLE I. Population analysis of the Pt_2–CO system calculated by the SAC/SAC-CI method.

	C						O					
	s	p_x	p_y	p_z	p_{tot}	Charge	s	p_x	p_y	p_z	p_{tot}	Charge
Adsorbed System $1A_1$[a]	3.188	0.697	0.645	0.917	2.259	0.330	3.742	1.552	1.435	1.341	4.328	−0.099
Separated System $1A_1$[b]	3.771	0.520	0.523	1.034	2.077	−0.010	3.727	1.437	1.436	1.379	4.252	0.018
Separated System $1A_2$[b]	3.754	0.486	0.487	1.051	2.024	−0.066	3.709	1.467	1.468	1.381	4.316	0.074
Separated System $1B_1$[b]	3.754	0.486	0.487	1.051	2.024	−0.066	3.709	1.467	1.468	1.381	4.316	0.074

	Pt											
	s	p_x	p_y	p_z	p_{tot}	d_{xx}	d_{yy}	d_{zz}	d_{xy}	d_{xz}	d_{yz}	d_{tot}	Charge
Adsorbed System $1A_1$[a]	0.528	0.095	0.017	0.044	0.156	1.139	1.382	1.293	1.953	1.706	1.960	9.433	−0.116
Separated System $1A_1$[b]	0.107	0.015	0.014	0.015	0.044	1.313	1.286	1.282	1.988	1.988	1.994	9.852	−0.003
Separated System $1A_2$[b]	0.600	0.033	0.014	0.017	0.064	1.249	1.313	1.304	1.490	1.988	1.996	9.340	0.004
Separated System $1B_1$[b]	0.599	0.032	0.017	0.018	0.067	0.991	1.188	1.191	1.987	1.987	1.995	9.339	0.005

[a]For the bridge adsorption geometry. The Pt_2–C distance of 1.44 Å is used for the adsorbed system.
[b]The Pt_2–C distance of 4.8 Å is used for the separated system. These states are the lowest ones of the A_1, A_2, and B_1 symmetries (see Fig. 6).

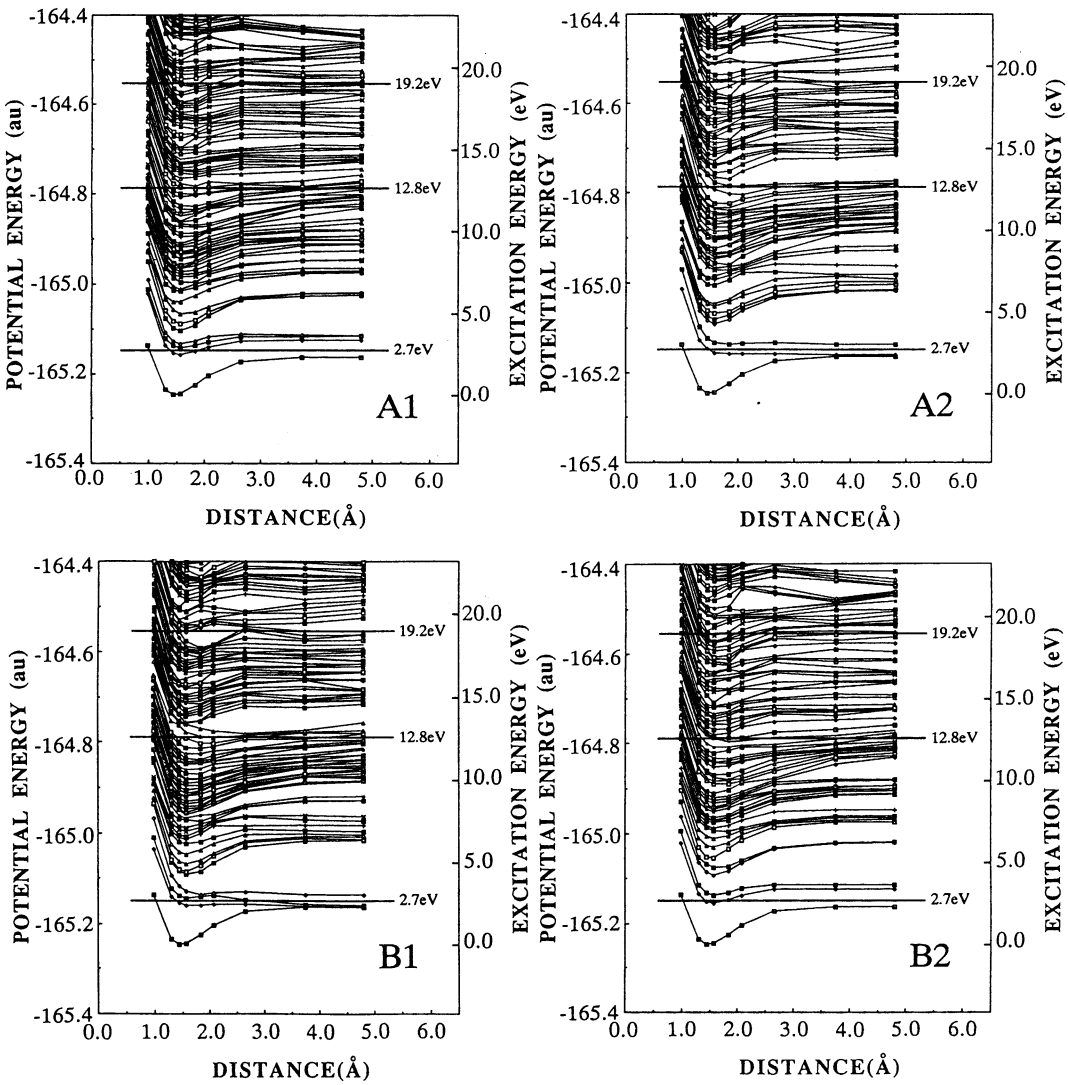

FIG. 3. Adiabatic potential energy curves for the ground and excited states of Pt_2–CO (bridge structure) calculated by the HF/SECI method for the A_1, A_2, B_1, and B_2 symmetries. The ground state having A_1 symmetry is shown for all the symmetries for comparison.

and most of the excited states have bound shapes, except for the lower ones in the A_2 and B_1 symmetries. From the analysis of main configurations, we found that most of the excited states are due to excitations within the metal. It is difficult to imagine a simple picture of the PSD from these dense PEC's.

We note that in the HF/SECI level, the electronic configuration of the platinum in the Pt_2–CO system is calculated to be close to $d^{10}s^0$, although the electronic configuration of the ground state Pt_2 should be close to d^9s^1, as shown in our previous calculation.[24] Therefore, at the SECI level, all the excited states in Fig. 3 have platinum d electrons between 19 and 20.

The nonadiabatic transitions occur easily when two PEC's are close in energy as seen in Fig. 3. The probability of the transition should be large between the electronic states having similar characters like those suffering the avoided crossing. Nicolaides *et al.* studies such nonadiabatic situations.[38–40] In the present study, we judge the characters of the calculated electronic states from the CI coefficients and connect the energy levels having similar characters, which gives nonadiabatic potential curves.

The nonadiabatic transition is often considered based on the nonadiabatic coupling[38–40] given by

$$\langle \Psi_A | \partial / \partial R | \Psi_B \rangle, \tag{1}$$

where Ψ_A and Ψ_B are the two adiabatic wave functions and R is the reaction coordinate. If this element is zero, the nonadiabatic transition between A and B states does not occur. Since the present reaction coordinate R and therefore the operator $\partial/\partial R$ have A_1 symmetry, only the transitions between the states having same symmetry are possible. Although symmetry mixing may be caused by the rotation of CO, the rotational temperature of the desorbed CO is observed lower than the kinetic and vibrational ones in the PSD of CO/Pt.[5] Therefore, we do not consider in this paper the nonadiabatic transitions between the states having different symmetries.

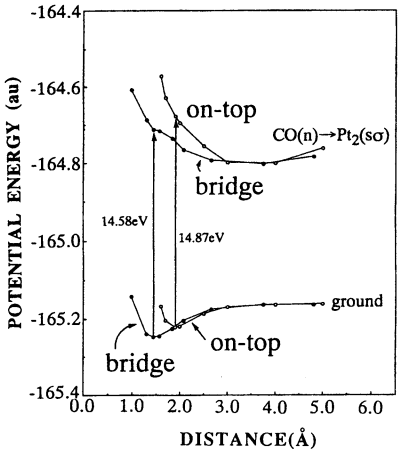

FIG. 4. Nonadiabatic potential energy curve calculated by the SECI method for the excited state having the nature of the $CO(n)\rightarrow Pt_2(s\sigma)$ excitation in its main configuration. The results for the bridge and on-top structures are compared.

Figure 4 shows the nonadiabatic PEC's of the excited states characterized by the excitation from the σ_b orbital, which is originally the n orbital of CO, to the σ_a orbital, which is mainly the $6s\sigma$ orbital of Pt_2 (see Fig. 2). For convenience, we show the curves for both of the bridge and on-top structures. These curves are obtained at the SECI level and correspond to the charge transferred states from CO to Pt_2, so that they give CO^+ as a PSD product. The potential curve for the bridge geometry was obtained by connecting the excited states in Fig. 3 (A_1) having the main configurations characterized as above. It ranges from 38th to 49th adiabatic PEC's in the Pt_2–C distances from 0.98 to 4.80 Å, so that it undergoes eleven avoided crossings in this region.

Figure 5 is the adiabatic PEC's for the on-top structure calculated by the HF/SECI method. The left one corresponds to the A' symmetry and the right to the A'' symmetry. Comparing with Fig. 3, we see a large similarity, though the interaction is weaker generally in the on-top geometry than in the bridge form. In Fig. 4, we compare the ground state potentials calculated at the HF level for the two geometries. The upper curves are the non-adiabatic curves for the $CO(n)\rightarrow Pt_2(s\sigma)$ excitations. The nonadiabatic curves due to the $\sigma_b\rightarrow\sigma_a$ excitation are repulsive for both adsorption geometries and the excitation energies at the SECI level are 14.6 and 14.9 eV for the bridge and on-top structures, respectively.

We find no large differences between the on-top and bridge forms, though Fukutani *et al.*[11] reported that CO at the on-top site is 4 times more easily desorbed than that at the bridge site. If the on-top form is more strongly bound in the ground state (though the present calculation could not reproduce), the repulsive excited-state curve should be more strongly repulsive. The bridge-site CO lies closer to the Pt surface than the on-top site CO by about 0.47 Å, so that photonabsorption may be easier for the on-top CO. Except for these speculations, we find no essential differences between the CO's at the on-top and bridge sites. We therefore discuss in the following sections the adiabatic and nonadiabatic PEC's for the bridge adsorption form.

B. Excitations from 5*d* to 6*s* within Pt metal: Ground-state CO desorption

It is well known that electron correlations are very important for the excited states and for the system involving transition metals. Therefore we hereafter calculate the ground and excited states of the Pt_2–CO system by including electron correlations with the use of the SAC/SAC-CI method. The SECI solutions corresponding to the nonadiabatic states as shown in Fig. 4 are used as reference states in the configuration selection step of the SAC-CI calculations.

Figure 6 shows the PEC's of the ground and lower excited states of the Pt_2–CO system calculated by the SAC/SAC-CI method. The PEC's are adiabatic and not the nonadiabatic ones. In contrast to the PEC's at the HF/SECI level given in Fig. 3, the ground state of the Pt_2–CO system cal-

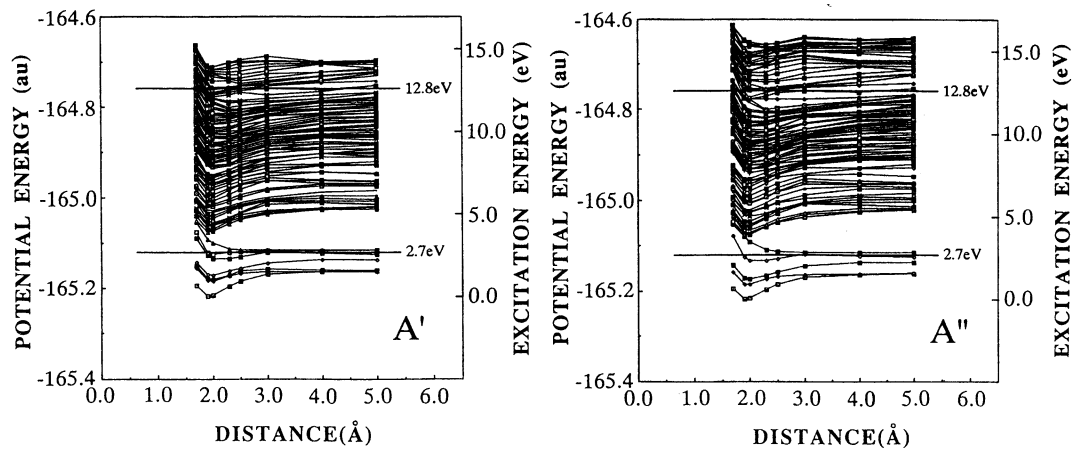

FIG. 5. Adiabatic potential energy curves for the ground and excited states of Pt_2–CO(on-top) calculated by the HF/SECI method for the A' and A'' symmetries. The ground state having A' symmetry is shown for all the symmetries for comparison.

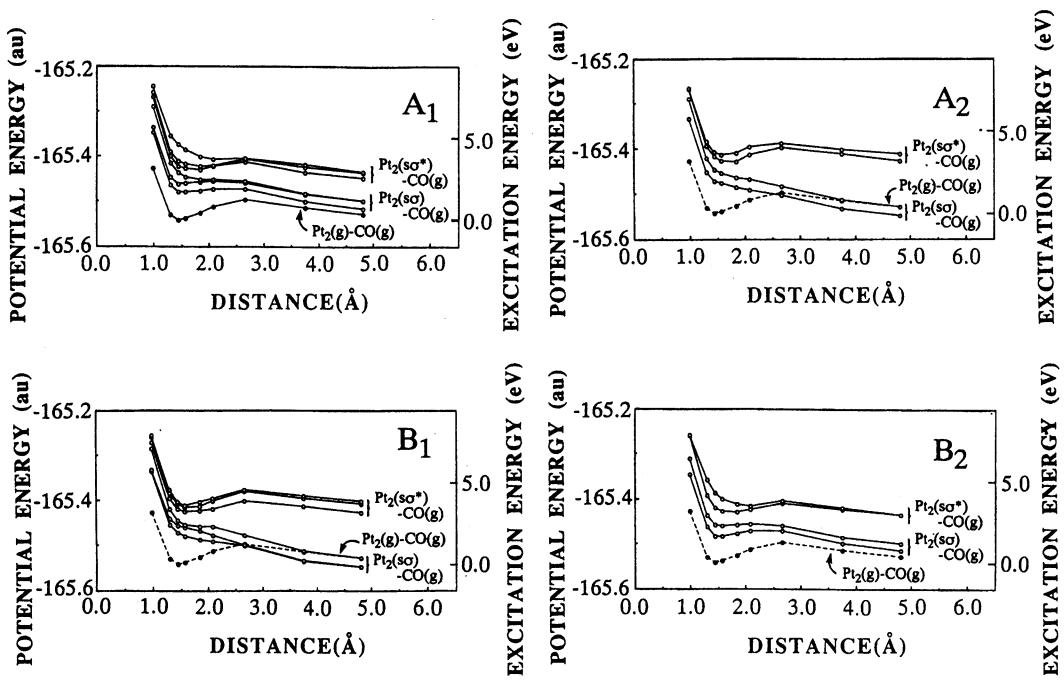

FIG. 6. Adiabatic potential energy curves for the lower states having A_1, A_2, B_1, and B_2 symmetries calculated by the SAC/SAC-CI method. The A_1 ground state is shown in all the figures.

TABLE II. Energies for the PSD of the CO molecule in the Pt_2–CO system compared with the experimental result and with those of free CO molecule.

		Adsorbed system				Free system	
Species	State	Main configuration	SAC-CI excitation energy (eV)	Threshold photon number[a]	Exptl.[a,b] threshold	SAC-CI excitation energy (eV)	Exptl.
CO (ground)		Pt_2 ($g\rightarrow e$)	1.6~2.6	1	2.7		
$CO^+(n)$	n-$1A_1$	0.75 ($n\rightarrow$Pt)	11.3	2	12.8	14.1	14.0
	n-$2A_1$	0.50 ($n\rightarrow$Pt)	12.8	2			
	n-$3A_1$	0.52 ($n\rightarrow$Pt)	14.8	3	19.2		
	n-$3B_1$	0.44 ($n\rightarrow$Pt)	14.6	3			
	n-$4B_1$	0.58 ($n\rightarrow$Pt)	15.3	3			
	n-$2B_2$	0.68 ($n\rightarrow$Pt)	14.0	3			
$CO^+(\pi)$	p-$1B_1$	0.62 ($\pi\rightarrow$Pt)	10.8	non		17.0	16.9
	p-$1B_2$	0.84 ($\pi\rightarrow$Pt)	10.6	non			
$CO^*(n\rightarrow\pi^*)$	n-$2B_1$	0.48 ($n\rightarrow\pi^*$)	12.7	2	19.2	9.0	8.5
	n-$1B_2$	0.61 ($n\rightarrow\pi^*$)	11.3	2			
$CO^-(d\rightarrow\pi^*)$	A_1	0.48 (Pt$\rightarrow\pi^*_{in}$)	7.6	2			
	A_1	0.58 (Pt$\rightarrow\pi^*_{out}$)	7.1	2			
	A_2	0.64 (Pt$\rightarrow\pi^*_{in}$)	8.2	2			
	A_2	0.48 (Pt$\rightarrow\pi^*_{out}$)	6.2	1			
	B_1	0.77 (Pt$\rightarrow\pi^*_{in}$)	7.2	2			
	B_1	0.43 (Pt$\rightarrow\pi^*_{out}$)	6.6	2			
	B_2	0.51 (Pt$\rightarrow\pi^*_{in}$)	6.8	2			
	B_2	0.81 (Pt$\rightarrow\pi^*_{out}$)	6.7	2			
$CO^-(\pi^*)$	$^1B_1$	0.97 (Pt$\rightarrow\pi^*$)	4.0(9.6)[c]	2			
	$^1B_2$	0.96 (Pt$\rightarrow\pi^*$)	3.4(9.1)[c]	2			

[a]Experimental photon energy is $1h\nu$=6.4 eV, $2h\nu$=12.8 eV, and $3h\nu$=19.2 eV.
[b]References 6, 7, and 11.
[c]Value in the parentheses is the sum of the electron attachment energy and the work function of the platinum surface.

TABLE III. Net charge of CO in the ground and lower excited states due to the $d \rightarrow s,p$ transition within Pt_2. SAC/SAC-CI results.

State	Net charge of CO	
	$R=1.44$ Å[a]	$R=4.80$ Å
$1\,^1A_1$(ground)	+0.231	+0.006
$2\,^1A_1$	+0.247	+0.008
$3\,^1A_1$	+0.219	+0.007
$4\,^1A_1$	+0.223	+0.007
$5\,^1A_1$	+0.299	+0.006
$6\,^1A_1$	+0.184	+0.006
$7\,^1A_1$	+0.158	+0.006
$1\,^1A_2$	+0.226	+0.008
$2\,^1A_2$	+0.209	+0.007
$3\,^1A_2$	+0.179	−0.001
$4\,^1A_2$	+0.228	+0.006
$1\,^1B_1$	+0.233	+0.008
$2\,^1B_1$	+0.230	+0.008
$3\,^1B_1$	+0.206	+0.008
$4\,^1B_1$	+0.183	+0.006
$5\,^1B_1$	+0.160	+0.010
$6\,^1B_1$	+0.212	+0.005
$1\,^1B_2$	+0.228	+0.007
$2\,^1B_2$	+0.210	+0.008
$3\,^1B_2$	+0.170	+0.006
$4\,^1B_2$	+0.195	+0.006

[a]The equilibrium distance of the Pt_2–CO system in the ground state.

culated by the SAC/SAC-CI method is the $^1A_2$ and $^1B_1$ states at larger Pt_2–CO distances: the $^1A_2$ and $^1B_1$ PEC's cross the $^1A_1$ PEC near $R=2.7$ Å. This crossing is due to the change in the ground electronic state of Pt_2 as a function of R. As seen from Table I, the population of Pt_2 in the $^1A_2$ and $^1B_1$ states are both $s^{1.2}p^{0.1}d^{18.7}$ at $R=4.80$ Å, and those in the $^1A_1$ state at $R=R$ eq. is $s^{1.0}p^{0.3}d^{18.9}$ so that if we trace the true ground state PEC, the changes in the populations are quite smooth. We have shown previously[24] that the ground state of a free Pt_2 has the configuration $d^{18}s^2$. In contrast, the populations of the $^1A_1$ state is $s^{0.2}p^{0.1}d^{19.7}$ when CO is separated.

Similar change in the electronic state of the Pt metal as a function of the metal-adsorbate distance was reported for the Pt–H_2 system (see Fig. 3 of Ref. 24) and for the Pt–CO system reported by Smith and Carter.[15] In both cases, the ground state of the adsorbed system is singlet $^1A_1$, but that of the separated system is triplet (the ground state of the Pt atom is ^{3}D).

In comparison with the PEC's in the HF/SECI level given in Fig. 3, the lowest state of the A_1 symmetry, which has been referred to as the "ground state," has a barrier of about 1 eV on the potential curve shown in Fig. 6. This barrier may be due to the aforementioned change in the electronic state of Pt_2 as a function of R. Since such change would be dependent on the size of the Pt_n cluster used in the calculations, this barrier may be due to the smallness of the present cluster model. We therefore discuss in the followings only some general features of the PEC's.

We see from Fig. 6, particularly from the A_2 and B_1 curves, that some lower excited states at $R=1.44$ Å are repulsive for the Pt–CO interaction. When the ground state of the Pt_2–CO system absorbs a photon of the energy of 1.6~2.6 eV, the CO molecule feels the repulsive force from the surface and is desorbed along this PEC. The translational temperature of the desorbed CO may be high, but the rotational temperature should be cool, as actually observed.[6,7]

This result means that there are the PSD channels just as proposed in the original MGR model. These PSD channels give the ground state CO molecule. At the potential minimum of the ground state of Pt_2–CO, the excitation energy for the desorption is 1.6~2.6 eV, which is lower than the experimental energy of 2.7 eV for the CO desorption from the Pt(111) surface. This result is summarized in Table II. We note that the excitations to the B_1 and B_2 states are optically allowed, at least in this model.

The main configurations of these repulsive states are the excitations from the $5d$ orbitals to the $6s$ and $6p$ orbitals of Pt: the excitations are within Pt_2, and CO itself is always in the ground state. The $5d \rightarrow 6p$ excited states are higher than the $5d \rightarrow 6s$ ones, but they mix strongly at shorter Pt_2–CO distances. At larger Pt–C distances, Pt_2 may be in the ground state or in the $d \rightarrow s$ or $d \rightarrow s^*$ state. We note that the energy levels of the $s\sigma$ and $s\sigma^*$ MO's are reversed at the Pt–C distances shorter than 2.08 Å, since the $6s\sigma$ MO has an antibonding interaction with the n MO of CO. Therefore, the configurations involving the $6s\sigma$ and $6s\sigma^*$ MO's mix strongly at shorter Pt–C distances.

The aforementioned analysis of the main configuration clearly shows the electronic mechanism of the PSD giving the ground-state CO. As shown in Fig. 2, the CO chemisorption on platinum is due to the σ donation of the n electron of CO to the vacant s and/or p orbitals of Pt and the π back donation from the occupied d orbital of platinum to the π^* orbital of CO. The $d \rightarrow s$ and $d \rightarrow p$ transitions within Pt_2 are, therefore, clearly unfavorable for the chemical bond formation between Pt_2 and CO, and lead to the desorption of CO from the Pt surface. We call this mechanism "unlock" mechanism, since the $d \rightarrow s,p$ transition within Pt_2 is just like unlocking the binding of CO from the metal-surface side.

The analysis of the electronic mechanism clearly implies that this excitation of a Pt metal, which is effective for the PSD giving the ground state CO, should be quite local: it should occur at the small region (or cluster) of the Pt surface or at that Pt atom which directly interacts with the CO molecule. Note that the $d \rightarrow s$ transition is optically forbidden, but the $d \rightarrow p$ transition is allowed, although the interaction with CO makes the $d \rightarrow s$ transitions to be optically allowed.

At the equilibrium Pt_2–C distance the excited states shown in Fig. 6 are located in the energy range from 1.6 to 4.5 eV, which is larger than the dissociation energy of the Pt_2–CO bond in the ground state.

Table III gives the net charge of CO at the Pt_2–C distances of 1.44 and 4.80 Å for the various lower states shown in Fig. 6. At 1.44 Å, the net charges of CO are all positive, and the differences from that of the $1\,^1A_1$ state are only from −0.073 to +0.068. At larger Pt_2–C distances, the net charge of CO decreases and becomes zero at 50.0 Å for all the states, which corresponds to the neutral CO desorption.

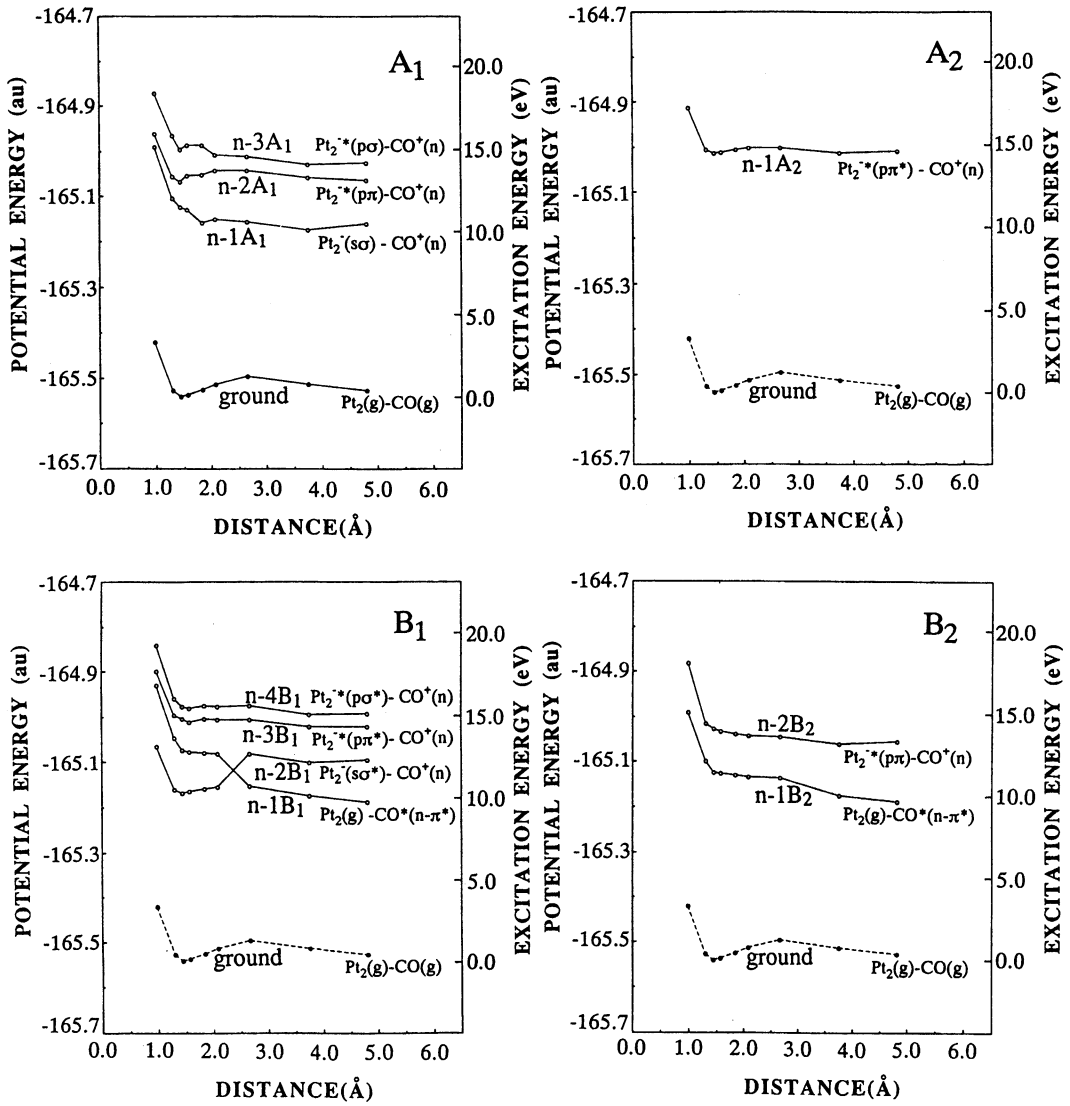

FIG. 7. Nonadiabatic potential energy curves for the excited states having A_1, A_2, B_1, and B_2 symmetries due to the excitations from the σ_b MO. The potential energies are calculated by the SAC/SAC-CI method. On the right-hand side, the electronic structures of Pt_2 and CO in the separated limit are shown. The ground state having the A_1 symmetry is shown in all the figures.

C. Excitations from the σ_b orbital: CO^+ and CO* desorptions

Figure 7 shows the nonadiabatic PEC's of the excited states due to the excitations from the σ_b orbital, which is the bonding orbital between the n orbital of CO and the s orbital of Pt_2, to the lower 10 unoccupied MO's, which consist mainly of the $6s$ and $6p$ orbitals of Pt_2 and the π^* orbital of CO. They are calculated by the SAC-CI method. At the Pt–C distance of 4.80 Å, these excited states have an ionic structure $Pt_2^- - CO^+(n)$ or the neutral structure Pt_2–CO* with the CO in the excited $n \rightarrow \pi^*$ state. All the CO^+ have the electron hole in the n orbital [it is therefore denoted as $CO^+(n)$] and the electron transferred to Pt_2 occupies the $6s$ and $6p$ orbitals of Pt. The asterisk on CO means it is in the excited state. In Fig. 7, n-$3B_1$, for example, denotes the third B_1 state having the nature of the excitation from the n orbital of CO. On the right-hand side of Fig. 7, we show the PSD product which is expected to be obtained along that nonadiabatic potential curve. As seen from Fig. 7, the lower two curves having B_1 symmetry exchange their natures.

Almost all the nonadiabatic PEC's shown in Fig. 7 are essentially repulsive. This implies that there are the MGR-type PSD channels in the excited states leading to the cationic species $CO^+(n)$ and the neutral excited species $CO^*(n \rightarrow \pi^*)$. These MGR-type repulsive curves are, however, nonadiabatic and embedded in the dense adiabatic curves shown in Fig. 3, most representing the excitations within the metal. The MGR-type process in this case is actually a series of nonadiabatic transitions between the neighboring adiabatic states having a similar nature for which the non-adiabatic coupling given by Eq. (1) is large. This is different from the lower-energy MGR process giving the ground-state CO discussed in the previous section.

The lowest-excited-state nonadiabatic curve with the A_1

TABLE IV. Net charge of CO at two different Pt_2–CO distances for the excited states due to the excitations from the σ_b MO. SAC/SAC-CI results.

Nonadiabatic state	Net charge of CO		Charge of CO as PSD product
	$R=1.44$ Å[a]	$R=4.80$ Å	
$1\,^1A_1$(ground)	+0.231	+0.006	neutral
n-$1A_1$	+0.290	+0.992	cation
n-$2A_1$	+0.184	+0.988	cation
n-$3A_1$	+0.223	+0.709	cation
n-$1A_2$	+0.620	+1.000	cation
n-$1B_1$	+0.543	+0.024	neutral
n-$2B_1$	+0.352	+0.985	cation
n-$3B_1$	+0.314	+0.962	cation
n-$4B_1$	+0.487	+0.953	cation
n-$1B_2$	+0.294	+0.007	neutral
n-$2B_2$	+0.472	+0.991	cation

[a]The equilibrium distance of the Pt_2–CO system at the ground state.

symmetry, denoted as n-$1A_1$ in Fig. 7, corresponds to the curve given in Fig. 4 and has the excitation character, σ_b to σ_a, so that it leads to CO^+. On the other hand, the curve for the n-$1B_1$ and n-$1B_2$ states lead to the neutral separated system, Pt_2 and CO*, where Pt_2 is in the ground state and CO is in the $^1\Pi(n\rightarrow\pi^*)$ excited state. At the Pt–C distance of 4.80 Å, the energy difference between the n-$1B_1$ and n-$1B_2$ states is only 0.003 eV. In Fig. 7, the other nonadiabatic curves given by the solid lines lead to $CO^+(n)$ and Pt_2^-. The ground state of Pt_2^- has an excess electron in the $s\sigma$ orbital (n-$1A_1$ state) and the other Pt_2^- has an excess electron in higher orbitals.

Table IV displays the net charge of CO at two different Pt_2–C distances for the nonadiabatic states shown in Fig. 7. At $R=1.44$ Å, the net charges of CO are all positive, ranging from +0.18 to +0.62, and most are larger than that of the ground state, +0.213. As the Pt_2–C distance increases, the positive charges increase up to unity except for the nonadiabatic states, n-$1B_1$ and n-$1B_2$, for which the net charge of CO decreases to zero. This charge of CO corresponds to the charge of CO obtained as the PSD product along the corresponding nonadiabatic PEC's shown in Fig. 7.

The lowest curve leading to CO^+ is curve 1 for the n-$1A_1$ state in Fig. 7, and the electronic structures of the PSD product, CO^+ and Pt_2^-, are in their ground states. At the Pt_2–C distance of 1.44 Å, the equilibrium distance of the ground state, the excitation energy for this state is calculated to be 14.9 and 11.3 eV by the HF/SECI and SAC/SAC-CI methods, respectively, where the latter result is of course more reliable than the former. The calculated excitation energy of 11.3 eV is lower than the twice of the photon energy (6.4 eV) used in the PSD experiment. We think that this is the origin of the second-order dependence on the laser fluence for the CO^+ desorption.[6]

In Table II, we summarize the excitation energies by which the CO^+ PSD processes are initiated. They are 11.3–15.3 eV which correspond twice to thrice of the photon energy, 6.4 eV, used in the experiment.

The PSD channels giving the $^1\Pi(n\rightarrow\pi^*)$ excited state of CO exist along the nonadiabatic curves for the n-$1B_1$ and n-$1B_2$ states. At distances larger than 2.66 Å, the energy levels of the two states are degenerate. However, at distances shorter than 2.66 Å, the situation is a bit complicated: the configurations corresponding to the excitation $\sigma_b\rightarrow\pi_a$ are distributed among the n-$1B_2$, n-$2B_2$, n-$2B_1$, and n-$4B_1$ states. The main configuration of the n-$1B_1$ state is the excitation within Pt_2 at distances shorter than 2.66 Å. Thus, the excitations to the n-$1B_2$, n-$2B_2$, n-$2B_1$, and n-$4B_1$ states at the ground state equilibrium distance would lead to the PSD product, $CO^*(\sigma_b\rightarrow\pi_a)$, and the excitation energies to these states are calculated to be 11.3, 14.0, 12.7, and 15.3 eV, respectively, by the SAC-CI method. These excitation energies are about 2–2.5 times of the photon energy (6.4 eV) used in the PSD experiment. This brings the second- and third-order dependencies on the laser fluence, while the experimental dependence was third order.[6] Though the experiment did not identify the electronic state of the desorbed CO, we propose it to be the $n\rightarrow\pi^*$ excited state.

As shown in Fig. 7, the upper curves have the nature of $Pt_2^-+CO^+$. The reneutralization of this CO^+ would also give neutral CO, which would be in the ground state. This mechanism was considered by Peremans *et al.*[6]

The repulsive nature of the nonadiabatic PEC's shown in Fig. 7 is easily understood from the nature of the main configurations of the excited states. They represent the excitations from the σ_b MO, which is the bonding orbital between n orbital of CO and s orbital of Pt_2, to either of the s or p orbital of Pt_2 or the π^* orbital of CO. The former ones lead to CO^+ with a positive hole on the n orbital, and the latter ones lead to the $n\rightarrow\pi^*$ excited state of CO. Since the σ_b orbital is strongly bonding between Pt_2 and CO, the excitation from this orbital leads to the desorption of CO.

In Fig. 7, the nonadiabatic PEC's giving the ionic separated system slightly rise up from 3.75 to 4.80 Å. This is due to the electrostatic interaction between CO^+ and Pt_2^- or the image force depending on $\sim 1/R$, which is caused by the charge-transfer excitation. However, in the shorter range, the origin of the surface-molecule interaction is not due to the image force, but due to the more chemical interactions as represented by the donation and back donation between CO and Pt_2. These chemical interactions are described by the short-range forces depending exponentially on R like two-center overlap integrals.

The present result does not support the Antoniewicz model[14] for the PSD and electron stimulated desorption (ESD), although it may be possible for physisorbed systems. Although the model assumes an existence of the charged species generated by the photon absorption, the charge on the adsorbate is not large enough when the surface-adsorbate distance is small, since at such distances the adsorbate electron cloud is embedded in the surface electron cloud.

D. Excitations from the π_n orbital

Next, we investigate the excitations from the π_n MO, which is mainly the bonding π orbital of CO but is almost nonbonding for the metal–CO interaction (see Fig. 2). Figure 8 shows the nonadiabatic PEC's of the states due to the ex-

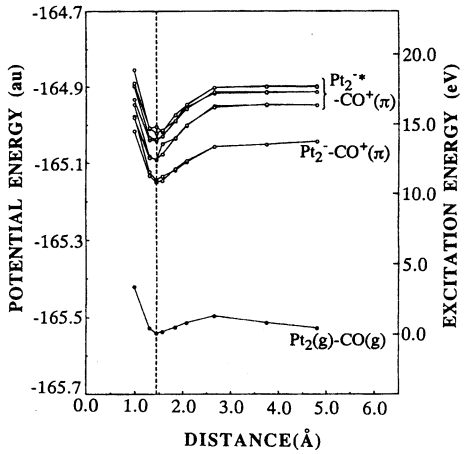

FIG. 8. Nonadiabatic potential energy curves for the excited states due to the excitations from the π_n MO. The potential energies are calculated by the SAC/SAC-CI method.

TABLE V. Net charge of CO at the two different Pt_2–CO distances for the excited states due to the excitations from the π_n MO. SAC/SAC-CI results.

Nonadiabatic state	Net charge of CO	
	$R=1.44$ Å[a]	$R=4.80$ Å
$1\,^1A_1$(ground)	+0.231	+0.006
p-$1B_1$	+0.465	+1.001
p-$2B_1$	+0.690	+1.009
p-$3B_1$	+0.729	+1.005
p-$4B_1$	+0.379	+1.005
p-$2B_2$	+0.717	+1.001
p-$2B_2$	+0.664	+0.982
p-$3B_2$	+0.499	+0.959
p-$4B_2$	+0.716	+1.004

[a]The equilibrium distance of the Pt_2–CO system at the ground state.

citations from the π_n orbital to the s and p orbitals of Pt_2. Only the $^1B_1$ and $^1B_2$ excited states are shown, but those having $^1A_1$ and $^1A_2$ symmetries are similar to those of Fig. 8. These PEC's are nonadiabatic and obtained by connecting the excited states having similar main configurations.

All the excited-state nonadiabatic PEC's shown in Fig. 8 are bound and the potential minima exist around 1.44 Å. Since the π_n MO's do not participate to the Pt_2–CO bonding interaction, but are localized on CO, the excitations from the π_n MO's do not affect the bonding between CO and Pt_2 and therefore the PEC's show bound natures as the ground state one. The excited states from π_n to π_a MO's, which are not shown in Fig. 8, are also bound. The bound energies estimated from these PEC's are larger than 3 eV. We therefore conclude that the excitations from the π_n orbital do not lead to the PSD.

The nonadiabatic PEC's of the excited states shown in Fig. 8 are connected with the ionic separated system, $Pt_2^- + CO^+$, where the cation CO^+ has a hole in the π MO, and an electron is transferred to the $6s$ and $6p$ orbitals of Pt_2. Since CO π cation is an excited cation, it may relax to lower states, e.g., n cation or neutral CO, on the surface.

Table V shows the net charge of CO at different Pt_2–C distances. At 1.44 Å, the positive charge of CO ranges from +0.379 to +0.717 but at 4.80 Å, it is about +1 corresponding to CO^+. We note that the positive charges in Table V are larger than those in Table IV, since the π_n orbital is more localized on CO than the σ_b MO.

One may wonder whether the Antoniewicz-type PSD may occur in this case since both the ground and excited states are bound. An essence of the Antoniewicz model is that the equilibrium surface-adsorbate distance is shorter in the excited *charged* state because of the image force. In the present case, the excited states are certainly charged as shown in Table V, but the calculated potential minima for the excited states are very similar to that of the ground state. Even in this typical ionic system, the bond between Pt_2 and CO is due to an ordinary chemical interaction (like σ donation and π back donation in this case) and the electrostatic interaction like image force is small. Thus, the Antoniewicz model does not apply to the present system.

E. Excitations giving CO^- as a PSD product

We next study the PSD channels giving CO^- as a desorption species. Figure 9 shows the nonadiabatic PEC's for the excitations from the Pt d orbitals to the π_a orbitals, the electron transfer excitations from metal to CO giving CO^-. Two curves correspond to the lowest excitations to the in-plane and out-of-plane π_a orbitals. The ground-state curve is also given. The upper curves are not repulsive but have a shallow bound nature. In this system, the σ donation is larger than the π back donation (see Sec. III), so that the excitations to the π_a orbitals little affect the attractive Pt_2–CO interaction. The excitation energies at the ground-state minimum are summarized in Table II. They lie in the range of 6.2–8.2 eV: one to two photon energy region of the 193 nm (6.4 eV) laser. Since the minima of the upper potentials are shallow, the PSD can occur when the system gains enough excess energy.

Table VI shows the population analysis of the CO molecule in these excited states at the Pt_2–CO distance of 1.44 and 4.80 Å. Note that these states at 1.44 Å are not anionic but rather cationic, although most of these states are more anionic than the ground state. However, at 4.80 Å, all of these states are well characterized as CO^- from the population analysis. The desorption species is certainly CO^-. This shows that the interaction between Pt_2 and CO is strong and the charge-transfer character of the excited states is rather small at small Pt_2–CO distances. This result is similar to the case of the CO^+ desorption.

Other excitations giving CO^- are the excitations of the bulk-metal electron to the π_a orbital. They are represented in the present model by the anion system $(Pt_2\text{–}CO)^-$. The PEC's for this anion system are given in Fig. 10. They are similar to those in Fig. 9 but bound nature is less prominent.

The electron attachment energy calculated at the ground state minimum is 3.4–4.0 eV. Adding the work function of the platinum surface, 5.65 eV,[41] the energy is calculated to be 9.1–9.6 eV, which is larger than the aforementioned values.

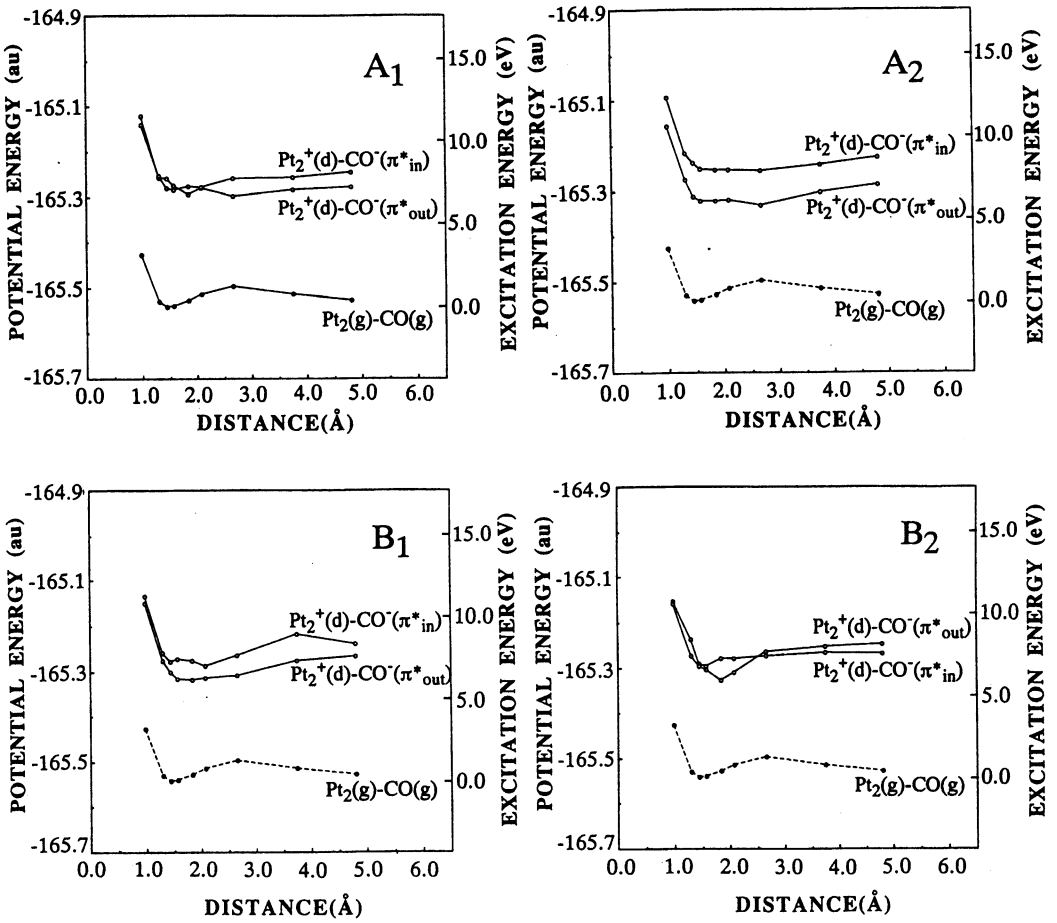

FIG. 9. Nonadiabatic potential energy curves for the excited states due to the excitations from the $Pt_2(d)$ to π_a MO. The potential energies are calculated by the SAC/SAC-CI method.

This is because the electron-hole attractive energy which exists in the previous case is much smaller in the present case: it is included only as a image force correction. Thus, the electron giving CO^- is supplied from the Pt_2 directly interacting with CO rather than from the bulk metal.

In conclusion, the two model studies show that the PSD giving CO^- (π anion) would also occur on the Pt surface. Since there are shallow minima in the excited-state PEC's, the lifetime of the excited species would be larger than those giving CO^+, for example. This would be observed through the rotational temperature etc. of the desorbed CO^- species.

TABLE VI. Net charge of CO in the ground and the excited states due to the $d \rightarrow \pi_a$ transition calculated by the SAC/SAC-CI method.

Symmetry		Net charge of CO	
	π_a	$R=1.44$ Å[a]	$R=4.80$ Å
$1\,^1A_1$(ground)		+0.231	+0.006
A_1	in-plane	+0.240	−0.990
	out-of-plane	+0.199	−0.852
A_2	in-plane	+0.226	−0.390
	out-of-plane	+0.128	−0.699
B_1	in-plane	+0.217	−0.872
	out-of-plane	+0.229	−0.909
B_2	in-plane	+0.220	−0.911
	out-of-plane	−0.006	−0.818

[a]The equilibrium distance of the Pt_2–CO system in the ground state.

V. COMPARISON OF THE DIFFERENT PSD PROCESSES

We have shown in this study four kinds of PSD products from different channels; namely, the ground state CO, the cation CO^+, the excited state CO*, and the anion CO^-. Table II is a summary of the excitation energies of the Pt_2–CO system. The excitation energies of a free CO are also given. The electronic structure of the desorbed cation CO^+ should be n cation and not a π cation, and that of the desorbed CO* molecule should be in the $n \rightarrow \pi^*$ excited state and not in the $\pi \rightarrow \pi^*$ excited state. The anion CO^- should be in its ground state. While the previous experimental studies[3–7] have shown that both neutral and cation CO molecules are led by the PSD, and that CO^- may be involved in the PSD process, the electronic structures of the desorbed CO and CO^+ have never been clarified. We hope such the experimental study be done in near future.

The excitation energy necessary for the PSD channels giving neutral CO is calculated to be 1.6~2.6 eV by the

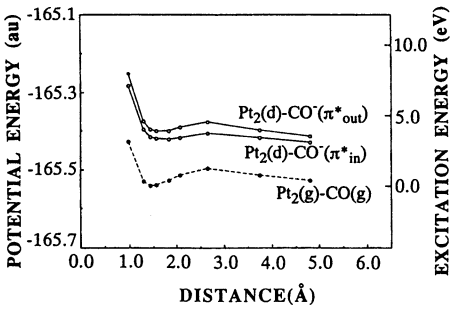

FIG. 10. Nonadiabatic potential energy curves for the electron-attachment to π_a MO. The potential energies are calculated by the SAC/SAC-CI method.

SAC/SAC-CI method in comparison with the experimental energy threshold of 2.7 eV. This channel involves the $5d \rightarrow 6s$ excitation of Pt_2. Even in an actual extended surface, this excitation should be quite local in the sense that this $5d \rightarrow 6s$ excitation should occur on those Pt atoms that are interacting with CO. This is because the repulsive nature of the excited states is due to a loss of the σ donation and the π back donation interactions between CO and Pt whose $5d$ and $6s$ AO's are involved. The binding due to the metal $5d$ and $6s$ AO's are "unlocked" by the $5d \rightarrow 6s$ transition.

The PSD channels giving a cation CO^+ and an excited state CO* are clarified. The cation should be n-hole cation and the excited state should be $n \rightarrow \pi^*$ one. This is because the repulsive natures of the non-adiabatic excited states are due to a loss of the σ donation interaction by these excitations. The energy ranges for the PSD channels giving CO^+ and CO* are calculated to be 11.3–15.3 and 11.3–12.7 eV, respectively, by the SAC-CI method as shown in Table II. These energy ranges correspond to two to three photons and two photons, respectively, of the experimentally used photon of 6.4 eV.

The excitations giving the CO cation having a hole in the π orbital are shown not to have the PSD channels, though the excitation energies are calculated to be 10.6–10.8 eV. This is because the π orbital is well localized on CO and has almost nothing to do with the bonding with the Pt metal.

The anion species CO^- (π anion) would also be desorbed by photoirradiation. They are produced by the electron-transfer excitations from the metal d orbital (or the bulk electron) to the π_a orbital localized on CO. The excitation energy lies in the range of 6.2–8.2 eV; one to two photon energy of the 193 nm (6.4 eV) laser. Since the upper nonadiabatic PEC's have shallow minima in this case, the lifetime of the CO^- species would be larger than those of CO^+, for example, affecting the rotational temperature, etc.

It is interesting to compare the excitation energies of CO on the Pt surface and in its free state. In the free system, the ionization potentials giving the n and π cations of CO are 14.0 and 16.9 eV, respectively. The SAC-CI results are close to the experimental values. On a Pt surface, the system would be stabilized at least by the work function of Pt which is 5.65 eV,[41] and therefore, the cation should be formed with less energy on the surface than in a gas phase. We see this trend in Table II. Furthermore, on the surface, the π cation is formed with less energy than the n cation, although the reverse is true in a gas phase. This is mainly due to the stabilization of the σ_b MO on the surface (see Fig. 2), while the π_n orbital is localized and therefore not stabilized.

On the other hand, for the neutral excited states, the stabilization due to the work function is not expected. Furthermore, the excitation energy within CO would become large when CO interacts with the surface as expected from Fig. 2. Thus, the $n \rightarrow \pi^*$ excitation energy of CO is larger on the surface than in a gas phase, as shown in Table II.

We have shown in this study that the MGR model is valid as the PSD processes as giving the ground state CO, n cation CO^+ and the $n \rightarrow \pi^*$ excited state of CO. Except for the ground state case, the upper repulsive curves in these MGR processes are nonadiabatic. There are no simple repulsive curves in the adiabatic picture: the important relevant states are embedded in the metal excited-state bands. The PSD occurs through a sequential nonadiabatic transitions among such relevant states: by connecting such states, we get the nonadiabatic PEC's.

The present calculations have clearly shown that the interaction of CO with a Pt surface is due essentially to the chemical bond formed by the σ donation and π back-donation type interactions. Even when the charged species CO^+ is involved as an excited state, the image force is secondary and our PEC's are quite different from those assumed by Antoniewicz. The repulsive nature of the upper curves in the MGR-type PSD processes are due to a loss or breaking of the metal-adsorbate bond existed in the ground state. Thus, the PSD's of CO from the Pt surface are quite chemical processes.

We conclude that the present study successfully clarifies the electronic mechanisms of the PSD of the CO molecule from a Pt surface. It explains some features observed by the experiments, but from experiments alone, it is almost impossible to clarify the detailed mechanisms occurring on the surface. The present study has served to clarify such mechanisms of the PSD of CO on a Pt surface. We have chosen the present CO/Pt system because it is a prototype system related to the rapidly growing field of surface photochemistry. The success of the present study, together with that of the previous study on the harpooning, surface chemiluminescence, and electron emission in the Cl_2/K, Na, and Rb systems,[29] encourage us to apply our methodology to various surface photochemistry.

ACKNOWLEDGMENTS

The calculations have been carried out with the computers in our laboratory and at the Computer Center of the Institute for Molecular Science. Part of this study was supported by the Grant-in-Aid for Scientific Research from the Ministry of Education, Science, and Culture of Japan.

[1] X-L. Zhou, X-Y. Zhu, and J. M. White, Surf. Sci. Rep. **13**, 73 (1991).
[2] K. Mase, S. Mizuno, M. Yamada, I. Doi, T. Katsumi, S. Watanabe, Y. Achiba, and Y. Murata, J. Chem. Phys. **91**, 590 (1989).

[3] K. Fukutani, A. Peremans, K. Mase, and Y. Murata, Phys. Rev. B **47**, 4007 (1993).
[4] K. Fukutani, A. Peremans, K. Mase, and Y. Murata, Surf. Sci. **283**, 158 (1993).
[5] K. Fukutani, M.-B. Song, and Y. Murata, Faraday Discuss. Chem. Soc. **96**, 105 (1993).
[6] A. Peremans, K. Fukutani, K. Mase, and Y. Murata, Phys. Rev. B **47**, 4135 (1993).
[7] A. Peremans, K. Fukutani, K. Mase, and Y. Murata, Surf. Sci. **283**, 189 (1993).
[8] Y. Murata and K. Fukutani (private communication).
[9] X. Guo, J. Yoshinobu, and J. T. Yate, Jr., J. Chem. Phys. **92**, 4320 (1990).
[10] P. Kronauer and D. Menzel, in *Adsorption-Desorption Phenomena*, edited by F. Ricca (Academic, New York, 1972), pp. 313–328.
[11] J. A. Pybyla, H. W. K. Tom, and G. D. Aumileer, Phys. Rev. Lett. **68**, 503 (1992).
[12] D. Menzel and R. Gomer, J. Chem. Phys. **41**, 3311 (1964).
[13] P. A. Redhead, Can. J. Phys. **42**, 886 (1964).
[14] P. R. Antoniewicz, Phys. Rev. B **21**, 3811 (1980).
[15] G. W. Smith and E. A. Carter, J. Phys. Chem. **95**, 2327 (1991).
[16] H. Nakatsuji, J. Chem. Phys. **87**, 4995 (1987).
[17] H. Nakatsuji, H. Nakai, and Y. Fukunishi, J. Chem. Phys. **95**, 640 (1991).
[18] H. Nakatsuji and K. Hirao, J. Chem. Phys. **68**, 2035 (1978).
[19] H. Nakatsuji, Chem. Phys. Lett. **59**, 362 (1978); **67**, 329 (1979); **67**, 334 (1979).
[20] H. Nakatsuji, Chem. Phys. **75**, 425 (1983).
[21] H. Nakatsuji, Acta Chim. Hungarica, **129**, 719 (1992).
[22] H. Nakatsuji and H. Hada, J. Am. Chem. Soc. **107**, 8264 (1985); **109**, 1902 (1987).
[23] H. Nakatsuji, M. Hada, and T. Yonezawa, Surf. Sci. **185**, 319 (1987).
[24] H. Nakatsuji, Y. Matsuzaki, and T. Yonezawa, J. Chem. Phys. **88**, 5759 (1988).
[25] H. Nakatsuji and Y. Fukunishi, Int. J. Quantum Chem. **42**, 1011 (1992).
[26] H. Nakatsuji and H. Nakai, Chem. Phys. Lett. **174**, 283 (1990).
[27] H. Nakatsuji and H. Nakai, Can. J. Chem. **70**, 404 (1992).
[28] H. Nakatsuji and H. Nakai, J. Chem. Phys. **98**, 2423 (1993).
[29] H. Nakatsuji, R. Kuwano, H. Morita, and H. Nakai, J. Mol. Catal. **82**, 211 (1993).
[30] H. Nakatsuji, M. Hada, K. Nagata, H. Ogawa, K. Domen, and J. Kondo, J. Phys. Chem. **98**, 11 840 (1995).
[31] H. Nakatsuji, M. Yoshimoto, M. Hada, K. Domen, and C. Hirose, Surf. Sci. **336**, 232 (1995).
[32] K. P. Huber and G. Hertzberg, *Molecular Spectra and Molecular Structure, IV. Constants of Diatomic Molecules* (Van Nostrand Reinhold, New York, 1979).
[33] L. E. Sutton, *Tables of Interatomic Distances and Configuration in Molecules and Ions* (Royal Society of Chemistry, London, 1965).
[34] P. J. Hay and W. R. Wadt, J. Chem. Phys. **82**, 270 (1985).
[35] S. Huzinaga, J. Chem. Phys. **42**, 1293 (1965); T. H. Dunning, Jr., J. Chem. Phys. **53**, 2823 (1970).
[36] M. Dupuis and A. Farazdel, Program System HONDO8 from MOTECC-91 (1991).
[37] H. Nakatsuji, Program System for SAC and SAC-CI calculations, Program Library No. 146 (Y4/SAC), Data Processing Center of Kyoto University (1985); Program Library SAC85, No. 1396, Computer Center of the Institute for Molecular Science (1981).
[38] I. D. Patsalakis, G. Theodorakopoulos, C. A. Nicolaides, and R. J. Buenker, Chem. Phys. Lett. **185**, 359 (1991).
[39] I. D. Patsalakis, G. Theodorakopoulos, and C. A. Nicolaides, J. Chem. Phys. **97**, 7623 (1992).
[40] G. Theodorakopoulos, I. D. Patsalakis, and C. A. Nicolaides, Chem. Phys. Lett. **207**, 321 (1993).
[41] *Handbook of Chemistry and Physics* (CRC, Cleveland, OH, 1984).